UC Irvine
UC Irvine Previously Published Works

Title

Polarity reveals intrinsic cell chirality

Permalink

https://escholarship.org/uc/item/6115r3k4

Journal

Proceedings of the National Academy of Sciences of the United States of America, 104(22)

ISSN

0027-8424

Authors

Xu, Jingsong
Van Keymeulen, Alexandra
Wakida, Nicole M
et al.

Publication Date

2007-05-29

DOI

10.1073/pnas.0703153104

Copyright Information

Peer reviewed

Polarity reveals intrinsic cell chirality

Jingsong Xu*[†][‡], Alexandra Van Keymeulen*[§], Nicole M. Wakida[¶], Pete Carlton[‖], Michael W. Berns[¶], and Henry R. Bourne*[‡]

*Departments of Cellular and Molecular Pharmacology and [‖]Biochemistry and Biophysics, University of California School of Medicine, San Francisco, CA 94158; and [¶]Beckman Laser Institute, University of California, Irvine, CA 92612

Like blood neutrophils, dHL60 cells respond to a uniform concentration of attractant by polarizing in apparently random directions. How each cell chooses its own direction is unknown. We now find that an arrow drawn from the center of the nucleus of an unpolarized cell to its centrosome strongly predicts the subsequent direction of attractant-induced polarity: Of 60 cells that polarized in response to uniform f-Met-Leu-Phe (fMLP), 42 polarized to the left of this arrow, 6 polarized to the right, and 12 polarized directly toward or away from the centrosome. To investigate this directional bias we perturbed a regulatory pathway, downstream of Cdc42 and partitioning-defective 6 (Par6), which controls centrosome orientation relative to polarity of other cells. Dominant negative Par6 mutants block polarity altogether, as previously shown for disrupting Cdc42 activity. Cells remain able to polarize, but without directional bias, if their microtubules are disrupted with nocodazole, or they express mutant proteins that interfere with activities of PKCζ or dynein. Expressing constitutively active glycogen synthase kinase 3β (GSK3β) causes cells to polarize preferentially to the right. Distributions of most of these polarity regulators localize to the centrosome but show no left–right asymmetry before polarization. Together, these findings suggest that an intrinsically chiral structure, perhaps the centrosome, serves as a template for directing polarity in the absence of spatial cues. Such a template could help to determine left–right asymmetry and planar polarity in development.

asymmetry | migration | neutrophil

Blood neutrophils respond to inflammatory stimuli by adhering to vessel walls, crawling through the endothelium, and migrating toward sites of infection or tissue injury. To do so, they respond to external cues by taking on a polarized morphology, with pseudopods containing protrusive actin polymers and uropods containing contractile actomyosin. As is the case with neurons and budding yeast, neutrophil polarity may orient toward a gradient of external stimulus but can also be elicited by spatially uniform stimuli. In this "undirected" polarity, cells orient in apparently random directions but morphologically resemble cells responding to spatial cues.

Most studies of neutrophil polarity have focused on regulated actin assemblies rather than on microtubules, perhaps because a neutrophil's microtubules are necessary neither for polarity nor for directed migration (1–4) and their locations differ from those of microtubules in most migrating cells. In a polarized neutrophil, unlike an astrocyte, neuron, or fibroblast, the nucleus is located near the leading edge, directly behind the pseudopod, whereas the centrosome is located behind the nucleus, where it organizes microtubules predominantly directed toward the cell's back and sides (5), rather than toward the leading edge.

Despite these differences, we were intrigued by accumulating evidence that microtubules and the centrosome redistribute toward the leading edge of polarizing astrocytes, neurons, and fibroblasts (6–9) and a report (10) that the axon forms on the neuron's periphery preferentially at the site closest to the centrosome before polarization. Accordingly, we asked whether the orientation of undirected neutrophil polarity is biased by the relative locations of the centrosome and nucleus before application of a spatially uniform polarizing stimulus.

We find that the centrosome's location relative to the nucleus strongly biases the orientation of undirected polarity in neutrophil-like differentiated HL60 (dHL60) cells. The direction of bias is surprising: Cells polarize preferentially to the left of an arrow pointing from the center of the nucleus to the centrosome in the cell's unpolarized state. We infer that the unstimulated dHL60 cell is intrinsically chiral; that is, its structure includes a chiral template that uses two axes of prepolarization asymmetry, imposed by centrosome location and adherence to the coverslip, to orient left–right asymmetry of morphologic polarity along the third axis. Further studies indicate that this leftward bias requires microtubules and elements of the well studied Cdc42/partitioning-defective 6 (Par6) polarity-determining pathway.

Intrinsic chirality may be a property of all centrosome-containing cells in metazoan organisms and may therefore play important roles in planar polarity, asymmetric cell division, and development of left–right asymmetry in the embryo.

Results and Discussion

Leftward Bias of Polarity Induced by Uniform f-Met-Leu-Phe (fMLP). To ask whether centrosome location determines the direction of polarity, we observed polarization induced by uniform fMLP in dHL60 cells transiently expressing either of two fluorescent markers for the centrosome: GFP-tagged arrestin-3 (GFP-Arr3), which localizes in centrioles (5) or GFP-N-Clip170, which associates with growing plus-ends of microtubules (11, 12), thereby highlighting the centrosome, where most microtubules originate. Fig. 1 shows two cells that polarized either downward and to the right (Fig. 1*A*) or upward and to the left (Fig. 1*C*). Both cells, however, polarized to the left of the red arrows, drawn before fMLP stimulation (at time = 0 sec) that point from the centers of their nuclei to their centrosomes (see Fig. 1 *B* and *D*). Diagrams on the far right in Fig. 1 *B* and *D* show the locations of centrosomes after exposure to fMLP for 180 or 360 s (in *B* or *D*, respectively).

In these and subsequent experiments (Fig. 2*A*), we tested 68 normal cells. Of these cells, 42 polarized clearly to the left, and 6 polarized clearly to the right of the red arrow; 8 cells failed to polarize, and 12 polarized in vertical directions (up or down).
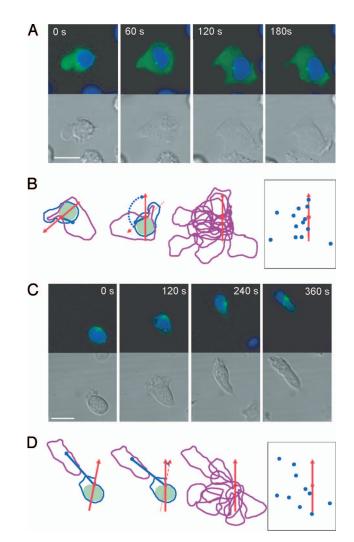
Fig. 1. Leftward bias of differentiated HL-60 (dHL-60) cell polarity. The bias of cell polarity was assessed by observing the locations of an individual cell's centrosome at two different times: before exposure to uniform fMLP by using GFP-Arr3 (*A* and *B*) or GFP-N- Clip170 (*C* and *D*) as markers and again when polarity was complete (180 or 360 s after application of fMLP in *A* and *B* or *C* and *D*, respectively). (*A*) dHL-60 cells were transiently transfected with GFP-Arr3 and uniformly stimulated with fMLP (100 nM) for the times indicated. GFP-Arr3 fluorescence (green) and nuclei (blue) are shown in the *Upper* images, and the corresponding Nomarski images are shown in the *Lower* images. (*B*) Leftward bias of cell polarity. In the first figure (far left), the cell outline from *A* is shown in blue (0 s) and purple (180 s after fMLP); centrosome positions are indicated by the red and blue dots (at 0 and 180 s, respectively) and are linked with a straight blue line; the red arrow is drawn through the center of the nucleus (light green), pointing to the centrosome, at 0 s. The second figure (second from the left) shows cell outlines and centrosome positions, at 0 and 180 s, rotated so that the arrow points directly upward. The third figure (second from the right) shows outlines of 13 GFP-Arr3 expressed cells at 180 s, all corrected so that their red arrows point in the same direction. The fourth figure (far right) shows the locations of centrosomes at 180 s. Only 1 of 13 cells polarized to the right side of the arrow. (*C*) (*Upper*) dHL-60 cells were transiently transfected with GFP-N-Clip170, and uniformly stimulated with fMLP (100 nM) for the times indicated. GFP-N-Clip170 fluorescence is green; nuclei are in blue. (*Lower*) The corresponding Nomarski images. (*D*) Outlines and centrosome positions of the cell in *C* at 0 and 360 s after fMLP addition are shown exactly as described in *B*. Of 11 GFP-N-Clip170-expressing cells, only 1 turned to the right of the arrow. (Scale bars, 10 μm.)

Thus, of the 48 cells whose direction could be reliably determined, 88% polarized to the left. These data are summarized in supporting information (SI) Table 1. As expected, the direction of polarity induced by uniform fMLP was random with respect to the frame of reference of the coverslip (SI Fig. 4).
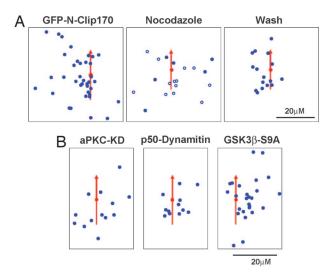

Fig. 2. Perturbing leftward bias. We assessed effects on leftward bias of perturbing either microtubules (*A*) or activities of three proteins thought to regulate polarity in other cells (*B*). (*A*) dHL-60 cells expressing GFP-N-Clip170 were subjected to no drug (*Left*), nocodazole (20 μM, 40 min) (*Center*), or 2 h after multiple washes with RPMI medium (*Right*), and then exposed to uniform fMLP (100 nM). Centrosome positions of the cells after polarization in response to fMLP are indicated by filled or empty blue circles, representing cells that expressed either of two centrosome markers, GFP-N-Clip170 or GFP-Arr3, respectively. For all GFP-N-Clip170-expressing cells, centrosome positions relative to the arrow were recorded at 360 s after exposure to fMLP, as described in the legend of Fig. 1*D*. Centrosome positions of GFP-Arr3-expressing cells (confined to the *Center* figure) were recorded at 180 s after exposure to fMLP, because these cells polarized more rapidly than cells expressing the other marker as described in the text. Thus the appropriate controls for the empty circles in this *Center* figure are the 13 GFP-Arr3-expressing cells whose positions after 180 s exposure to fMLP are depicted in Fig. 1*B*. Regardless of the centrosome marker used, the leftward bias of polarity was not detected after treatment with nocodazole (*Center*) but was restored after nocodazole was removed (*Right*). (Scale bar, 20 μm.) (*B*) dHL-60 cells were transiently cotransfected with GFP-N-Clip170 and one of following mutant constructs: PKCζ-KD (*Left*), p50-dynamitin (*Center*) GSK3β -S9A (*Right*), and then exposed to uniform fMLP (100 nM). Centrosome positions 360 s later were assessed as described in the legend to Fig. 1*B*. Whereas both PKCζ-KD and p50-dynamitin abolish the leftward bias, GSK3β -S9A reverses it. (Scale bar, 20 μm.)

The leftward bias of polarity required intact microtubules, as shown by the effect of disrupting microtubules with nocodazole (Fig. 2*A* and SI Table 1): The cells polarized and migrated in uniform fMLP, as reported in ref. 5, but polarized in random directions with respect to the locations of the centrosome and nucleus. Removal of nocodazole, which allowed microtubules to reassemble, restored the leftward bias (Fig. 2*A*).

Polarity Regulators Downstream of Cdc42: Par6, PKCζ, and Dynein. The leftward bias reveals that unpolarized dHL60 cells behave as chiral entities with three apparent axes of asymmetry (Fig. 3*A*): the nuclear–centrosomal axis, a vertical axis (from the cell surface adhering to the coverslip to the bathing medium), and a lateral axis that biases subsequent polarity to the left of the first axis. Because location of the centrosome relative to the nucleus relates intimately to the direction of polarity in other cells (6–10), we used drugs and dominant-interfering mutants to ask whether dHL60 polarity is controlled by a polarity pathway (Fig. 3*B*) that operates in neurons and astrocytes. The pathway's key upstream elements include Par6, a Rho GTPase called Cdc42, and either an atypical protein kinase C (aPKC) such as PKCζ (9, 13) or a different kinase, Akt (7), which is activated by phosphatidylinositol-3,4,5-*Tris*-phosphate (PIP3). A pivotal element
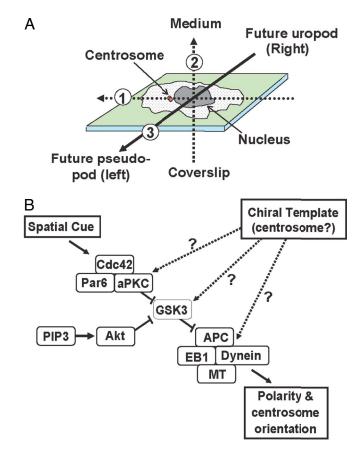
Fig. 3. Potential chirality axes (*A*) and possible regulators of leftward polarity bias (*B*). (*A*) Schematic diagram of an unpolarized cell resting on a coverslip, showing three chirality axes. Axis 1 is the arrow drawn from the center of the nucleus through the centrosome, and axis 2 is the vertical axis, from coverslip to medium. Orthogonal to the first two axes, axis 3 is the predicted direction of polarity to be assumed by the cell after addition of uniform fMLP: the pseudopod will be on the left, and the uropod will be on the right. (*B*) The diagram presents postulated relations among regulatory molecules we speculate may be involved in executing the leftward polarity bias of dHL60 cells. Solid lines connecting elements in the pathway represent steps documented in regulation of polarity and centrosome orientation in astrocytes and neurons (6–10). Dotted arrows with question marks indicate speculative links between a proposed chiral template and possible target steps in the pathway.

in the pathway is a constitutively active serine/threonine protein kinase, glycogen synthase kinase 3β (GSK3β), whose phosphorylation of a variety of downstream regulators appears to inhibit attachment of microtubules to structures at the leading edge of astrocytes and axons (6). This inhibition is reversed by phosphorylation of GSK3β at position 9, a conserved serine; PKCζ or Akt promote this phosphorylation, directly or indirectly (7, 9).

Disrupting upstream elements of the pathway, with dominant-negative Par6 mutants (14, 15), as well as mutants that disrupt function of Cdc42 or production of phosphatidylinositol-3,4,5-*Tris*-phosphate (PIP3) (16), prevented polarity altogether. Consequently, we cannot evaluate their possible roles in mediating directional bias. In contrast, interfering with two relatively downstream elements of the pathway randomized the direction of fMLP-induced polarity (Fig. 2*B*), abolishing the leftward bias. One was PKCζ: The direction of polarity was random in cells expressing a PKCζ mutant lacking kinase activity (Fig. 2*B* and SI Table 1) or treated with GF 109203X, a compound (17) that inhibits PKCζ and several other PKC isoforms (data not shown). A second was cytoplasmic dynein, a minus-end-directed micro-

tubule motor protein that is reported to anchor microtubules to the cell periphery (18). Overexpressing p50-dynamitin, which interferes with dynein function by disrupting the dynactin complex associated with it (19), produced an effect (Fig. 2*B* and SI Table 1) similar to that of interfering with PKCζ. (Note that 86% of normal cells, but only $\approx$60% of cells expressing either the PKCζ mutant or p50-dynamitin, were able to polarize. Cells expressing these constructs that were able to polarize, however, pointed in random directions with respect to the nucleus-to-centrosome arrow, quite unlike normal cells.)

Perturbing GSK3β Reverses the Leftward Bias of Polarity. GSK3β is perfectly positioned to act as a switch in the Cdc42/Par6 polarity pathway (Fig. 3*B*). In astrocytes, inhibition of GSK3β by activated upstream signals reverses its (constitutively) negative downstream effect on microtubule attachment to the cell periphery (14). Indeed, localized inhibition of GSK3β, resulting from its phosphorylation at Ser-9, is required for cultured neurons to form an axon. GSK3β phosphorylated at this position localizes specifically to the neurite destined to form an axon, and expression of GSK3β-S9A, a gain-of-function mutant that cannot be inhibited by phosphorylation, prevents axon formation (9, 20).

In dHL60 cells, GSK3β regulates a switch that controls the directional bias of polarity. Expression of GSK3β-S9A specifically reversed the direction of polarity in response to fMLP. Of 34 cells tested, 24 polarized: 2 cells polarized vertically, 4 polarized to the left of the nucleus-to-centrosome arrow, and 20 polarized to the right (Fig. 2*B* and SI Table 1). Like the leftward bias of normal cells, the rightward bias of GSK3β-S9A-expressing cells was abolished by nocodazole; that is, cells polarized in random directions, relative to the nucleus-to-centrosome axis (SI Fig. 5).

Inhibiting GSK3β with a selective inhibitor, SB216763 (21), had little or no effect on leftward bias (SI Fig. 5). In a sense, the lack of effect of SB216763 was to be expected, because the biochemically opposite manipulation (preventing inactivation of GSK3β by expressing GSK3β-S9A) produces a rightward bias. It is fair to note, however, that inhibiting either a putative upstream regulator (PKCζ) of GSK3β or putative downstream effectors (dynein, microtubules) randomizes the directional bias of polarization. If so, why does inhibiting GSK3β's catalytic activity not produce a similar randomizing effect? Our present knowledge does not allow us to resolve this question.

Because of its ability to reverse the leftward bias of polarity in response to uniform fMLP, we asked whether GSK3β-S9A selectively impairs the ability of chemotaxing cells to turn to the left in response to a leftward displacement of the source of chemoattractant. The mutant did impair the cells' ability to interpret gradients but showed no selective effect on their ability to turn left or right in response to shifting attractant cues (see *Effect of GSK3β-S9A on Chemotaxis* in SI Text and SI Fig. 6).

It seems likely that functional chirality of unstimulated dHL60 cells depends on asymmetric distribution of one or more key regulatory elements to the left or right of the nucleus-to-centrosome axis. Unfortunately, however, diligent efforts failed to find any such asymmetric distribution. The following elements showed no consistent asymmetry: the cell itself (nucleus and cytoplasm); number or mass of microtubules; Par6; dynein; PKCζ; dynactin; and GSK3β, unphosphorylated or phosphorylated at the S9 position (see *Subcellular Distribution of Polarity Regulators* in SI Text and SI Fig. 7).

Intrinsic Chirality and Centrosomes. We imagine that the dHL60 cell's chirality depends on a chiral structure, which serves as a template to determine the direction of polarization in response to uniform chemoattractant. One obvious candidate is the centrosome itself, which is inherited and chiral, as are its two

component centrioles (22). Laser-induced damage to the centrosome prevented polarization in response to uniform fMLP (see *Laser Ablation of the Centrosome* in [SI Text and SI Fig. 8](#)). The centrosome may be necessary for dHL60 polarity or, alternatively, the shock produced by acute centrosomal damage may simply poison the cell. Unfortunately, these results neither confirm nor rule out a role for centrioles or the centrosome as templates for functional cell chirality. Moreover, we do not know how centrioles, or any other chiral template, may control the putative pathway (Fig. 3B) that appears to "execute" leftward orientation of polarity, except that the GSK3β step in the pathway is an obvious candidate.

We strongly suspect, however, that intrinsic functional chirality is a property of eukaryotic cells, and probably confers selective advantage in the course of evolution. Chirality of individual neutrophils need not confer a selective advantage, of course, because these cells must interpret chemotactic gradients that may come from any direction *in vivo*; instead, intrinsic chirality is easier to detect in neutrophils, because we can induce them to polarize without furnishing spatial cues and under conditions where individual cells are free of interactions with their neighbors. Morphologic chirality, however, is a well established property of some protozoa (23) and of single-celled green algae such as *Chlamydomonas*, which exhibits radial asymmetry and dissimilar poles; the intrinsic chirality of *Chlamydomonas* is marked by structural features of the basal bodies (24), analogs of the mother centriole found at the base of primary cilia in mammalian cells.

Unlike neutrophils, many cells of metazoan organisms orient themselves in three dimensions during development, with orientations determined by contacts with adjacent cells and gradients of regulatory factors. An intrinsically chiral template could enhance a cell's prowess in multiple tasks that require integrating extrinsic inputs to organize asymmetric morphology, such as, for instance, in creating planar polarity and correct orientation of asymmetric cell division. The possibility that centrosomes or centrioles constitute such chiral templates is in keeping with phenotypes produced by mutations in inversin and other protein components of centrosomes, basal bodies, or primary cilia. Such mutations cause reversed or random left–right asymmetries in development, as well as polycystic kidneys and other defects in planar polarity and tissue organization (25–27). We note, however, that mutant *Drosophila* lacking centrioles are reported (28) to undergo nearly normal development, with some impairment of asymmetric cell division in neurons.

Materials and Methods

Antibodies and Reagents. Mouse polyclonal antibody against α-tubulin was purchased from Sigma (St. Louis, MO). Rabbit polyclonal antibody against phosphorylated GSK3β (Ser-9) was from Cell Signaling Technology (Beverly, MA). Rabbit polyclonal antibody against Par6 was a gift from Ian Macara (University of Virginia, Charlottesville, VA). Rabbit polyclonal antibodies against pericentrin and mouse monoclonal antibody against cytoplasmic dynein were purchased from Covance (Berkeley, CA). Mouse monoclonal antibody against p150[Glued] was from BD Biosciences (Franklin Lakes, NJ). Nocodazole and GF 10920X were from Calbiochem (San Diego, CA). SB216763

was purchased from Tocris Bioscience (Ellisville, MO) and fMLP was from Sigma.

Plasmids encoding GFP-N-Clip170 and p50-dynamitin were gifts from Ron Vale (University of California, San Francisco, CA). GFP-Arr3 was a gift from Marc Caron (Duke University, Durham, NC). GSK3β -S9A and -wt were gifts from Alan Hall (Sloan–Kettering Institute, New York, NY). PKC-KD was a gift from Martin Schwartz and Ian Macara (University of Virginia). The GSK3β-YFP and PKCζ-YFP fusions protein plasmids were constructed by cloning human GSK3β cDNA or PKCζ cDNA (obtained from Frederic Mushinski, National Cancer Institute, Bethesda, MD) into the pEYFP-N1 vector (Clontech, Mountain View, CA).

Cell Culture and Transfection. Cell culture of dHL60 cells and transfections were performed as described in refs. 16 and 29. For transient transfection, cells (on day 6 after the addition of DMSO) were washed once in RPMI medium 1640 Hepes and resuspended in the same medium to a final concentration of 10^8 ml^{-1}. DNA was then added to the cells (50 μg of GFP-N-Clip170 or GFP-Arr3 plasmid), and the cell–DNA mixture was incubated for 10 min at room temperature, transferred to electroporation cuvettes, and subjected to an electroporation pulse on ice at 310 V and low resistance. Transfected cells were allowed to recover for 10 min at room temperature and then transferred to 20 ml of complete medium. Subsequent assays were performed 4 h after transfection. For the indicated treatments with drugs, cells in suspension were exposed for 40 min to nocodazole (20 μm) or 1 h to SB126763 (10 μM) and allowed to adhere to dishes for an additional 20 min before the relevant perturbation or manipulation.

Chemotaxis Assays and Microscopic Analysis. For immunofluorescence analysis in fixed cells, cells were allowed to stick to fibronectin-covered coverslips and subjected to no stimulation or to stimulation with a uniform concentration (100 nM) of fMLP for 3 min, as described in refs. 16 and 29. Cells were fixed in 3.7% paraformaldehyde/0.25% glutaraldehyde or methanol and immunostained for α-tubulin or other desired proteins. Antibodies were used at a dilution of 1:100, and immunostaining was conducted as described in refs. 16 and 29.

Live cells were imaged after stimulation either with a uniform concentration of fMLP (100 nM) or exposed to a point source of attractant supplied by a micropipette (Femtotips) containing 10 μm fMLP as described in refs. 16 and 29. The migration path of each cell was assessed with SoftWorx software (Applied Precision, Issaquah, WA), as described in ref. 16.

1. Zigmond SH, Levitsky HI, Kreel BJ (1981) *J Cell Biol* 89:585–592.
2. Zigmond SH (1977) *J Cell Biol* 75:606–616.
3. Niggli V (2003) *J Cell Sci* 116:813–822.
4. Niggli V (2000) *FEBS Lett* 473:217–221.
5. Xu J, Wang F, Van Keymeulen A, Rentel M, Bourne HR (2005) *Proc Natl Acad Sci USA* 102:6884–6889.
6. Wiggin GR, Fawcett JP, Pawson T (2005) *Dev Cell* 8:803–816.
7. Jiang H, Guo W, Liang X, Rao Y (2005) *Cell* 120:123–135.
8. Gomes ER, Jani S, Gundersen GG (2005) *Cell* 121:451–463.
9. Cau J, Hall A (2005) *J Cell Sci* 118:2579–2587.
10. de Anda FC, Pollarolo G, Da Silva JS, Camoletto PG, Feiguin F, Dotti CG (2005) *Nature* 436:704–708.
11. Diamantopoulos GS, Perez F, Goodson HV, Batelier G, Melki R, Kreis TE, Rickard JE (1999) *J Cell Biol* 144:99–112.
12. Perez F, Diamantopoulos GS, Stalder R, Kreis TE (1999) *Cell* 96:517–527.
13. Etienne-Manneville S, Hall A (2003) *Nature* 421:753–756.
14. Etienne-Manneville S, Hall A (2001) *Cell* 106:489–498.
15. Tzima E, Kiosses WB, del Pozo MA, Schwartz MA (2003) *J Biol Chem* 278:31020–31023.

CELL BIOLOGY

16. Van Keymeulen A, Wong K, Knight ZA, Govaerts C, Hahn KM, Shokat KM, Bourne HR (2006) *J Cell Biol* 174:437–445.
17. Toullec D, Pianetti P, Coste H, Bellevergue P, Grand-Perret T, Ajakane M, Baudet V, Boissin P, Boursier E, Loriolle F, *et al.* (1991) *J Biol Chem* 266:15771–15781.
18. Dujardin DL, Vallee RB (2002) *Curr Opin Cell Biol* 14:44–49.
19. Schroer TA (2004) *Annu Rev Cell Dev Biol* 20:759–779.
20. Yoshimura T, Kawano Y, Arimura N, Kawabata S, Kikuchi A, Kaibuchi K (2005) *Cell* 120:137–149.
21. Coghlan MP, Culbert AA, Cross DA, Corcoran SL, Yates JW, Pearce NJ, Rausch OL, Murphy GJ, Carter PS, Roxbee Cox L, *et al.* (2000) *Chem Biol* 7:793–803.
22. Tassin AM, Bornens M (1999) *Biol Cell* 91:343–354.
23. Aufderheide KJ, Frankel J, Williams NE (1980) *Microbiol Rev* 44:252–302.
24. Geimer S, Melkonian M (2004) *J Cell Sci* 117:2663–2674.
25. Praetorius HA, Spring KR (2004) *Annu Rev Physiol*.
26. Singla V, Reiter JF (2006) *Science* 313:629–633.
27. Yokoyama T (2004) *Anat Sci Int* 79:47–54.
28. Basto R, Lau J, Vinogradova T, Gardiol A, Woods CG, Khodjakov A, Raff JW (2006) *Cell* 125:1375–1386.
29. Xu J, Wang F, Van Keymeulen A, Herzmark P, Straight A, Kelly K, Takuwa Y, Sugimoto N, Mitchison T, Bourne HR (2003) *Cell* 114:201–214.